Francesco Zardi, Payam Nayeri, Paolo Rocca, and Randy L. Haupt

Artificial Intelligence for Adaptive and Reconfigurable Antenna Arrays

A review.

This article provides an overview of a few applications of artificial intelligence (AI) in adaptive and reconfigurable antenna arrays. In particular, AI proves to be more robust than traditional approaches in noisy and high multipath environments compared to many signal processing algorithms. AI is highly dependent upon the array architecture and requires the signal control offered by digital beamforming. Five application areas are presented, including adaptive nulling, wireless localization, multiple-input, multiple-output (MIMO) communications, element failures, and calibration.

INTRODUCTION

The increasingly crowded and sometimes hostile radio spectrum requires communications and radar systems to adapt and reconfigure to the environment in which they operate. Adaptive arrays dynamically weigh and combine signals in a way that enhances the desired signal while rejecting interfering signals [1]. Adaptive arrays typically alter the antenna pattern by tuning the element weights in the software beamforming algorithms. A reconfigurable array alters the current distribution across its aperture to change its operating frequency, polarization, or radiation pattern. Reconfigurable arrays have either mechanically movable parts, switches, or other tunable components [2]. Adaptive and reconfigurable arrays have computer algorithms that guide their performance in a desired direction. Initially, these types of arrays relied on finite and infinite impulse response filters that found the weights through local optimization.

More recently, AI algorithms have enabled superior, fast global searches to find the element weights in real time. AI refers to "that activity devoted to making machines intelligent, and intelligence is that quality that enables an entity to function appropriately and with foresight in its environment" [3]. AI consists of "computational technologies that are inspired by—but typically operate differently from—the way people and other biological organisms sense, learn, reason, and take action" [4]. Machine learning (ML) algorithms enable AI by improving an outcome through experience. According to [5], ML approaches include:

- concept learning and general-to-specific ordering
- decision tree learning
- artificial neural networks (ANNs)
- evaluating hypotheses
- Bayesian learning
- computational learning theory
- instance-based learning
- genetic algorithms (GAs)

Digital Object Identifier 10.1109/MAP.2020.3036097
Date of current version: 2 December 2020

- learning sets of rules
- analytical learning
- combining inductive and analytical learning
- reinforcement learning.

These approaches use optimization, statistics, data searching, and interpolation to enhance human decision making.

AI algorithms are computer programs and are limited by the rules and skill of the people who wrote the code. As an example, a self-driving Uber car killed a pedestrian in Tempe, Arizona in March 2018 [6]. The ML algorithms were taught only to recognize a pedestrian in a crosswalk. In this situation, the pedestrian was not in a crosswalk, and the human inside the car was distracted on a smartphone. Some of the data collected in the AI decision making included signals from radar antennas. Another interesting situation occurred in September 1983 when the USSR early warning system detected incoming missiles from the United States [7]. The protocol required launching a USSR counterattack in retaliation to any launch by the United States. Fortunately, the duty officer, Stanislav Petrov, broke protocol and declared the warnings to be false alarms. An AI algorithm without human intervention would have followed the protocol with disastrous consequences. Human supervision of AI processes in antenna design and operation provides needed input when encountering unanticipated situations.

Examples of nature-inspired ML algorithms presented in this article model genetic evolution, animal swarm behaviors, and physical processes. For instance, GA and differential evolution (DE) use natural evolution/genetics and mutation [8]. In another example, particle swarm optimization (PSO) mimics swarm behavior in some groups of animals [9]. Finally, simulated annealing (SA) models the slow cooling of a molten substance into an optimum crystalline state [10].

In addition, this article explores the use of other important ML techniques applied to adaptive and reconfigurable arrays, such as radial basis functions (RBFs), support vector machines (SVMs), and ANNs. Deep neural networks (DNNs), a variation of ANNs with multiple layers, find solutions to very complex tasks with the proper training [11], [12].

Figure 1 indicates the recent spike in interest in the application of AI to adaptive and reconfigurable arrays. This figure displays the number of scientific articles published in IEEE journals in the last three decades. The survey was performed by counting the number of articles that matched the words "adaptive/reconfigurable antenna array," "direction of arrival," or "beamforming." Furthermore, only articles related to AI were considered by filtering keywords related to ML, such as "support vector machine," "machine learning," or "neural network," and those related to nature-inspired optimization techniques, such as "genetic algorithm," "particle swarm," or "simulated annealing."

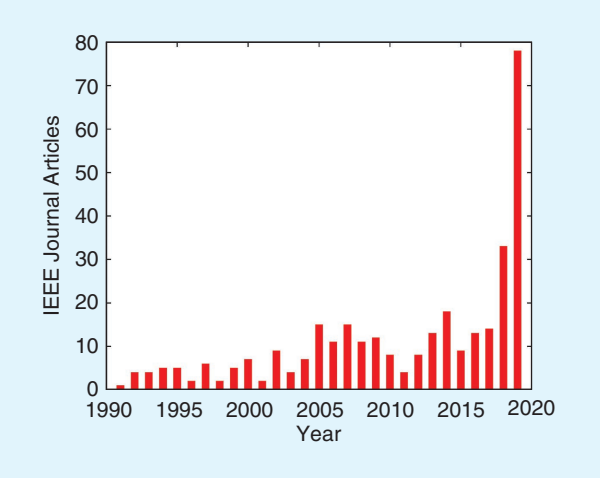

FIGURE 1. The publications on the topics of AI application to adaptive and reconfigurable arrays, direction finding, and beamforming.

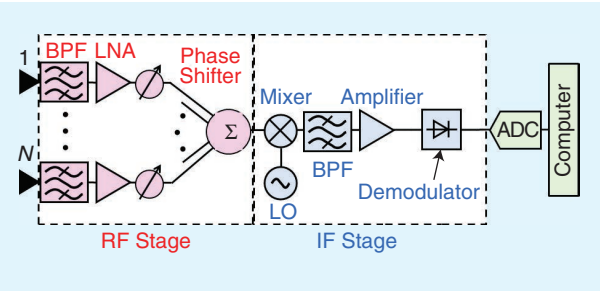

FIGURE 2. The radio frequency (RF) beamforming with an AESA architecture. BPF: bandpass filter; LNA: low-noise amplifier; LO: local oscillator; ADC: analog-to-digital converter; IF: intermediate frequency.

AI BEAMFORMING ARCHITECTURES

Since the 1960s, advances in electronics (transistors and integrated circuits) led a transition from passive to active arrays. The architecture of an *N*-element, active electronically scanning array (AESA) receiver appears in Figure 2 [13]. On receive, each element sends its received signal to components like BPFs, LNAs, and phase shifters. The modified output from each element sums to create one coherent beam at the output. This output is then down converted and amplified before being demodulated and sent to the ADC.

A reverse process exists for transmitting in which the computer sends bits to a digital–analog converter (DAC) before modulating, amplifying through a high-power amplifier (HPA), filtering, and upconverting the signal to a power splitter before the signals go to the elements. In the case of digital modulations, the signals (e.g., the IQ constellation) are created before the lowpass filter and ADC for receiving and before the HPA for transmitting. AESAs work well for standard beamforming, such as scanning the main beam and lowering the sidelobe levels. This type of architecture severely limits the adaptive and reconfigurable functions, though.

Adaptive nulling and DF arrays need to know the signal amplitude and phase at each element in the array to form an approximation of the signal covariance matrix used by various algorithms to determine the signal or interference directions [1]. The AESA RF beamforming architecture limits DF to periodograms that have poor resolution compared to the

superresolution algorithms possible with digital beamforming (DBF). Figure 3 depicts a DBF architecture that replaces the RF beamforming with software beamforming in the computer. DBF started gaining traction in the 1980s and struggled to gain acceptance until more recently [14], [15]. A DBF array ideally has an ADC for each element, but some designs place the ADC at the subarray output [16]. Transmitting arrays also make use of DBF.

Recent advancements in ADC/DAC technology eliminates the IF stage at each element of a DBF, enabling direct conversion transceivers. The direct conversion of an RF signal to bits

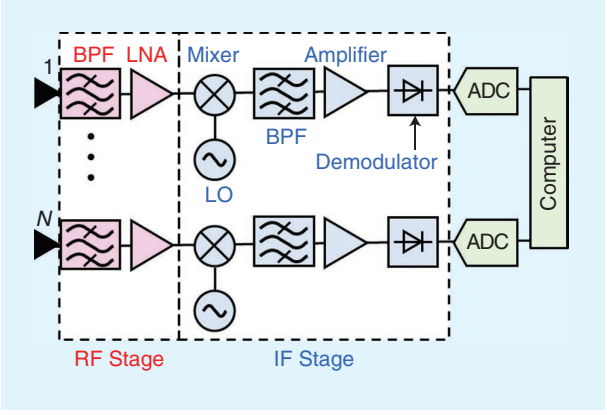

FIGURE 3. The DBF architecture.

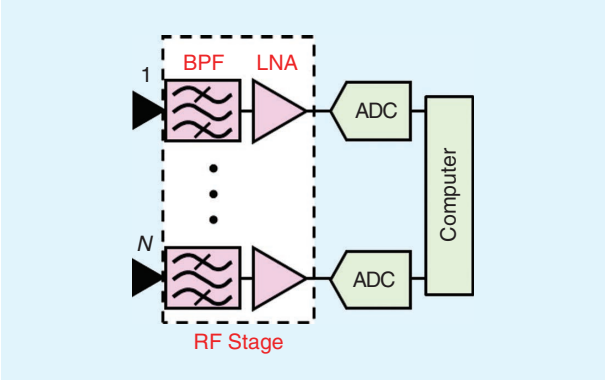

FIGURE 4. The direct conversion beamforming architecture.

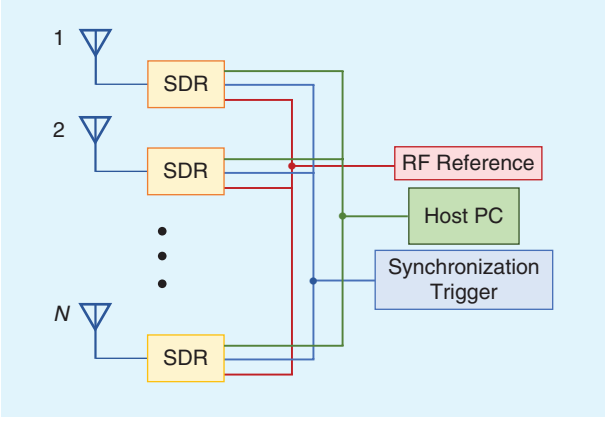

FIGURE 5. A block diagram of an SDR beamformer.

(Figure 4) has also enabled the use of a software-defined radio (SDR) at each element. Since each element has an SDR, the computer can not only perform adaptive nulling and DF but can also change waveforms and perform cognitive sensing of the environment [17]–[19].

AI APPLICATIONS FOR ADAPTIVE ARRAYS

This section presents five examples of state-of-the-art applications of AI for adaptive arrays.

ADAPTIVE NULLING

Adaptive nulling usually requires a DBF architecture and an algorithm that maximizes the signal-to-interference ratio. ML algorithms improve on this approach by having the ability to search beyond narrow corridors in the cost function and find success in very noisy and high multipath environments.

Adaptive nulling with a GA using an AESA architecture was first proposed in the 1990s [20]. Experimental results proved that ML was able to quickly place nulls in the antenna pattern of a cylindrical array by minimizing the total output power while using the least significant bits of the element weights [21].

Direct conversion beamforming offers many more opportunities to avoid interference compared to an AESA. An AI algorithm can not only place nulls in the antenna pattern but can frequency hop and change the waveform. A basic block diagram of the direct conversion beamformer with an SDR at each element is illustrated in Figure 5. The host PC controls the beamforming using an interference cancellation algorithm, while the RF reference and synchronization trigger calibrate and synchronize all SDRs.

Beamforming with an array of SDRs was first demonstrated in [18], and subsequent experimental studies using the beamformer were reported in [22]–[25]. Coherent beamforming requires synchronization of all of the SDRs in the array. A clock distributes a timing signal to synchronize the sample clocks and LO frequencies in each SDR [22]. While this approach synchronizes the array, it does not align the LO phase of each SDR device. The hardware setup in Figure 6 includes four National Instruments (NI) 2922 universal software radio peripherals (USRPs), one OctoClock-G CDA-2990 clock distribution accessory, and four monopole antennas. The USRPs interface with a host PC via an Ethernet switch.

Coherent beamforming requires calibrating the relative phases of the LOs and the relative amplitudes of the SDRs. One approach transmits a plane wave reference signal, as demonstrated in [25]. The calibration measures the difference in phase and amplitude received at each array element. One element signal serves as the reference used to correct discrepancies at the other elements. Another calibration approach sends a reference signal via a coaxial cable to each SDR receive port. Alternatively, the signal travels to a second receive port where the SDRs use the leakage between the receive ports to compare with the reference signal [26]. LabVIEW performed the initialization, calibration, measurement, and data processing in [22]–[25].

Experimental work on adaptive nulling interference cancellation with an SDR array was reported in [22]–[25]. Classic

adaptive nulling algorithms compare the received signal to an expected pilot signal and calculate the array weights that minimize the L2 norm of the difference between the received and expected signals [1]. Transmitters in realistic situations have a carrier frequency offset that is unknown at the receiver. In addition, in high-interference scenarios where the frequency of the received signal may not be distinguishable from the interference, classic adaptive algorithms cannot distinguish between the intended signal and the interference and will null the intended transmitter. Evolutionary algorithms offer a practical solution to resolve these issues.

Experimental adaptive nulling using a GA that controls an SDR array was reported in [25]. The four-element digital beamformer in Figure 6 received a desired signal from an NI USRP-2922 that was about 4 m away in the broadside direction. Two Signal Hound VSG25A transmitters created interference. All of the devices operated at 2.45 GHz. The experiments took place in a laboratory with significant multipath effects resulting from large metallic objects in close vicinity of the experiment.

Three different adaptive beamforming algorithms attempted to null the two interfering sources while receiving the desired signal. Sample matrix inversion (SMI) failed to cancel the interferences due to the carrier frequency offset problem. The second approach used a modified version of SMI that ignored the signal phase (i.e., it used only signal amplitude). In the third approach, a GA minimized the L∞ norm of the difference between the pilot signal and the array output signal. Bit error rates (BERs) were measured at different power levels using 4-quadrature amplitude modulation (4-QAM) for all three methods. The GA outperforms the other two techniques. Constellation plots of the received data using traditional SMI, modified SMI, and GA appear in Figure 7. In addition, Figure 7 illustrates the transmission of an uncompressed image in the presence of interference sources. Note that only the GA recovered the image in the presence of strong interference.

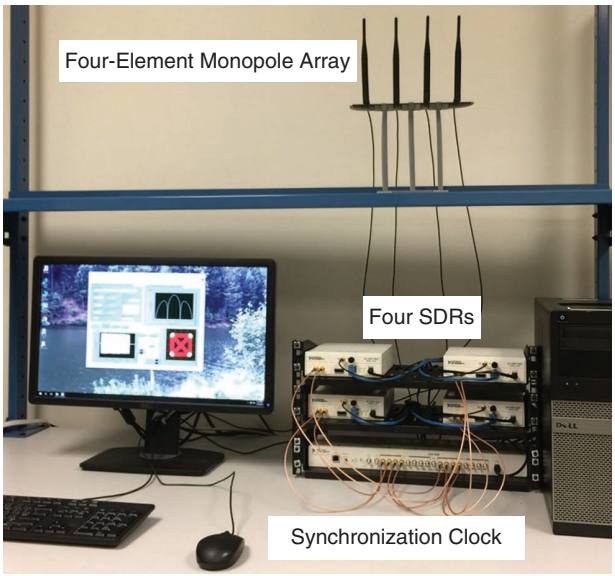

FIGURE 6. The hardware setup of the four-element software defined radio beamformer [18].

WIRELESS LOCALIZATION

Wireless localization finds the position of one or more desired targets. Position information is important for navigation, antenna siting, medical monitoring, and tracking. The approaches to wireless localization include proximity detection, triangulation, and signal property based [27]. DF determines the directions of sources arriving at an array using algorithms like multiple signal classification (MUSIC) [28] and estimation of signal parameters via rotational invariance techniques (ESPRIT) [29]. These superresolution algorithms have several drawbacks that are described in the next four paragraphs.

First, they require accurate modeling of the array patterns and the multipath propagation. Several AI approaches have been proposed that achieve increased robustness against imperfections in these models and element failures, for example, by employing RBF networks [30], DNN [31], [32] or support vector classification (SVC) [33].

Second, high-resolution signal subspace methods require many input samples, which may not be available in real-time applications, such as automotive or compact array systems. In these contexts, AI techniques such as SA [34] and multilayer perceptron (MLP) [35], [36] provide better results.

Third, AI techniques require a significantly smaller computational power for DF compared to methods employing eigenvalue decompositions [37]–[39]. In particular, Fuchs et al. show that a MLP architecture achieves performance on par with a maximum likelihood estimator and reduces the mean computation time from 1,500 to 1.5 ms [36]. Even single-layer ANNs have been demonstrated to achieve good performance using limited computational resources [40]. The reduced computational complexity is of particular interest in DF [33], [41].

Fourth, improvements on the mean-square error (MSE) of MUSIC estimates are possible, not only by replacing the well-known estimation methods [42] but also by combining these methods with AI techniques. Khan et al. investigated the possibility of enhancing the output of the MUSIC algorithm with various regression models, such as Gaussian processes (GPs), ANNs, and regression trees (RTs) [43]. As seen in Figure 8, the hybrid methods perform better than the original technique, in particular for the real scenario.

Table 1 compares the scenarios in which the previously mentioned DF techniques were tested. First, two types of DF problems can be identified, depending on the geometry of the employed antenna array, either linear (1D) or planar (2D). The 2D array geometry enables estimating both the elevation and azimuth direction of a source and typically results in a higher amount of data to process. It is possible to note from Table 1 that the DF methods dealing with a large number of sensors are mainly based on NN or DNN methods due to their ability to process large amounts of data in a fast and effective manner [12].

As for index evaluating the ratio between the number of simultaneous targets and the number of sensors (i.e., the

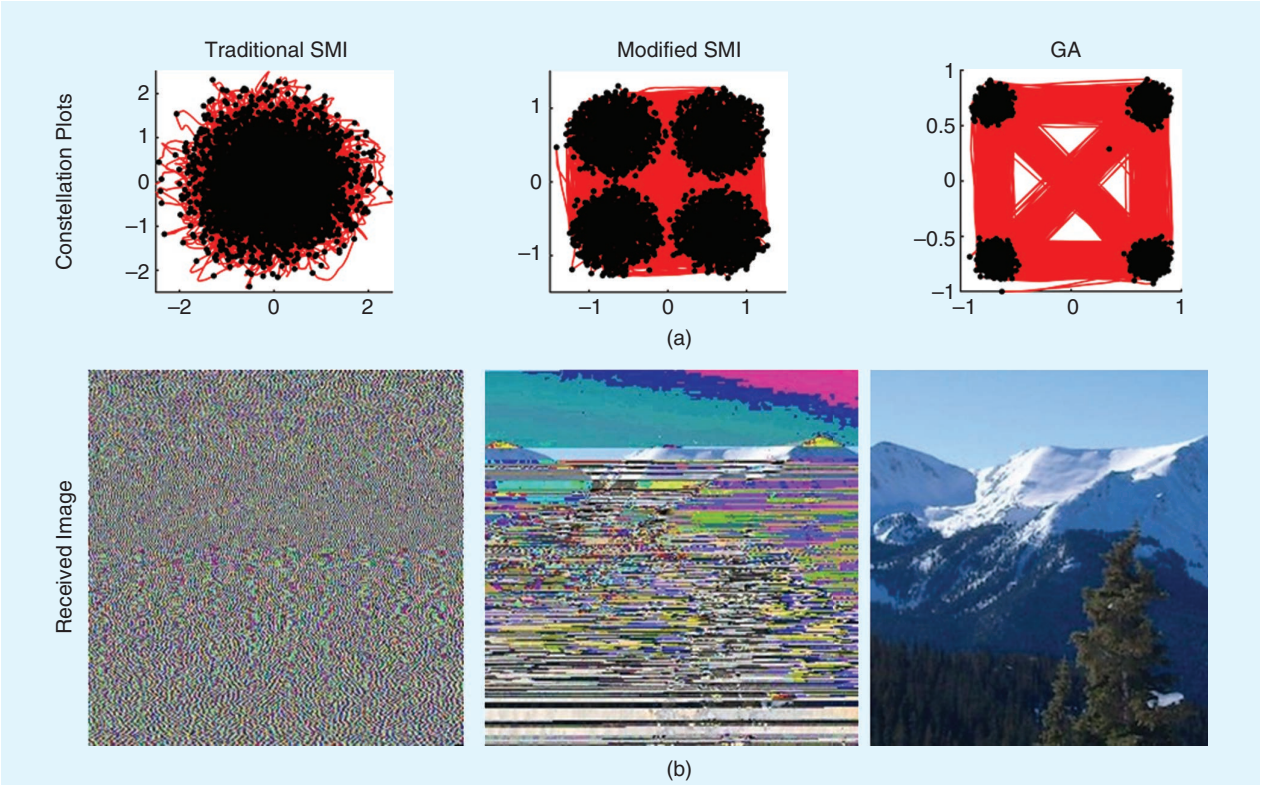

FIGURE 7. The constellation plots for the (a) received 4-QAM signal along with the (b) recovered images, received with three different interference cancellation algorithms: traditional SMI, modified SMI, and GA [25].

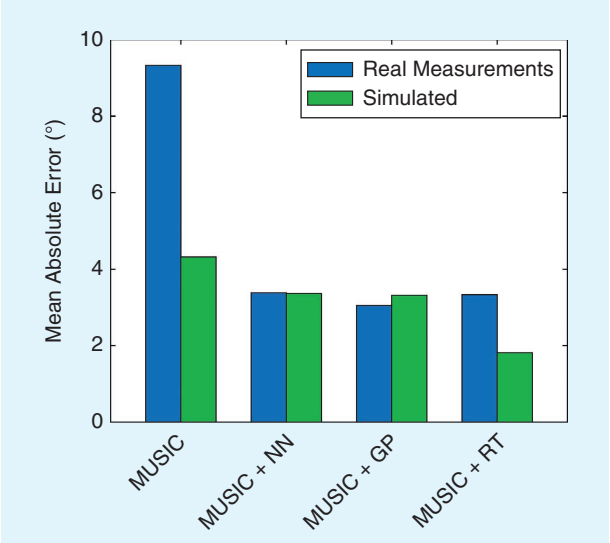

FIGURE 8. The DF estimation errors for different methods [43]. NN: neural network.

"Targets to Sensors Ratio" column of Table 1), it is possible to note that in only two cases, [33] and [36], this value is above 40%. Among them, only the DF method described in [33] allows for considering more targets than sensors, achieving a significantly higher ratio of 112.5% by means of a successful combination of SVC with probability mapping.

With reference to the "Signal-to-Noise" (SNR) column of Table 1, it is worth observing that many DF methods based on AI techniques are tested with very high noise levels, also in scenarios where the noise power exceeds the signal power. This outcome is in agreement with the well-known fact that ML-based methods present a remarkable robustness to noise and strong generalization capabilities [11], [12], [44].

In the framework of wireless localization, indoor wireless positioning and tracking cannot rely on global navigation satellite systems and must deal with strong multipath interference. In this context, highly distributed wireless sensor networks (WSNs) exploit the preexisting infrastructure, such as Wi-Fi access points [45]. An indoor experimental adaptive antenna, demonstrated in [46], used information regarding the presence of people in specific areas to select which of the appropriate transmitting antennas to use. In addition, a PSO-based technique described in [47] automatically inferred the position of nodes within a WSN.

AI techniques such as SVMs and convolutional neural networks (CNNs) have received significant attention, both in the case of active localization [48]–[50], where the target holds a device that sends a signal of some form, and device-free localization [51], [52], where the target does not hold a device. In

addition, the approach described in [53] achieves robustness against errors in the time synchronization and uncertainties in the location of the antennas using a Lagrange programming neural network.

MIMO COMMUNICATIONS

MIMO communication systems exploit arrays of antennas to increase the overall capacity of a system. The signals transmitted from the array elements undergo different paths through the channel due to spatial diversity. Channel state information (CSI) describes the signal distortions encountered in the channel. By exploiting diversity and using CSI, the receiving array elements can differentiate the signal components corresponding to the different transmitters. However, correctly estimating the CSI in a time-varying environment presents many challenges. Deep learning strategies for CSI estimation have proved to be very effective [54]–[57].

TABLE 1. A COMPARISON OF AI TECHNIQUES FOR DIRECTION FINDING.

Reference	AI Technique	Array Geometry	Number of Sensors	Number of Targets	SNR (dB)	Targets to Sensors Ratio (%)
[30]	RBF	1D	8	1	[5, 35]	12.5
[31]	DNN	1D	10	[1, 3]	10	30
[32]	DNN	1D	24	2	[–10, 10]	8.33
[33]	SVC	2D	16	[1, 18]	[20, 30]	112.5
[34]	SA	1D	8	3	10	37.5
[35]	MLP	2D	6	1	[9,12]	16.67
[36]	MLP	1D	4	2	[–3, 30]	50
[37]	MLP	2D	8	1	[–5, 5]	12.5
[38]	DNN	1D	128	32	[0,25]	25
[39]	SONFIN	1D	4	1	[–5, 25]	25
[40]	HNN	1D	10	3	[–2.5, 15]	30
[41]	MLP	2D	16	1	10	6.25
[42]	RBF-NN	1D	8	[1, 2]	[–5, 40]	25
[43]	ML	2D	4	1	[0, 30]	25

SONFIN: self-constructing neural fuzzy inference network; HNN: Hopfield neural network.

Deep learning approaches to CSI estimation are also capable of exploiting complex antenna architectures such as the continuous aperture phased (CAP) MIMO transceiver of Figure 9 [58]. This antenna architecture has P RF chains connected through a switching network to an array of N radiating elements, with $N > P$. A metamaterial lens in front of the array maps signals from different directions to different elements of the array, and vice versa. Despite the limited number of RF chains available, the deep learning approach presented in [59] provides an accurate estimate of the CSI, outperforming compressed sensing-based algorithms in terms of MSE.

Deep learning approaches have also been suggested for reducing the burden of sharing CSI information between uplink and downlink. In [60], a DNN was trained to compress CSI into an optimal representation for transmission between uplink and downlink. In two-tier heterogeneous MIMO networks, the CNN-based method described in [61] enables inferring the CSI information of an auxiliary traffic base station from the knowledge of the control base station CSI. Finally, a deep learning approach is employed in [62] to directly reconstruct the uplink CSI from the downlink channel information.

A comparative overview of the referenced state-of-the-art CSI estimation methods is given in Table 2. The majority of these techniques adopt DNN, and the reason for this outcome is twofold. First, DNNs are capable of tackling highly dimensional problems involving hundreds of unknowns, as in the case of CSI estimation of the channels between tens of antennas. Second, DNN can provide real-time results after an initial training phase, making them ideal for practical implementations in commercial devices.

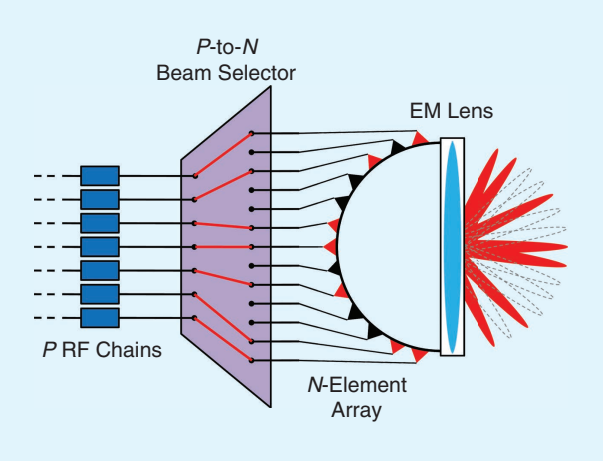

FIGURE 9. The CAP-MIMO antenna architecture for mm-wave beamspace communications [58]. EM: electromagnetic.

The data reported in Table 2 also demonstrate the existence of a variety of models for simulating MIMO communication channels. The availability of such models is of high interest for the development of AI since it enables the generation of large amounts of labeled data at a low cost. These vast training sets are valuable for the training of ML-based methods, in particular DNN architectures requiring the optimization of hundreds of weights.

It is worth noting that, while most of the methods reported in Table 2 assume that the noise power is smaller or equal to that of the received signal, the analysis performed in [56] considers SNR values down to –15 dB. Even in this extreme case, where the noise power is approximately 30 times stronger

TABLE 2. A COMPARISON OF AI TECHNIQUES FOR CSI ESTIMATION IN MIMO COMMUNICATIONS.

Reference	AI Technique	Number of Antennas at Base Station	Number of Antennas at Mobile Device	SNR (dB)	Channel Model	Application
[54]	DNN	64	16	[5, 25]	Block fading	CSI estimation
[55]	DNN	64	32	[10, 30]	Beamspace MIMO	CSI estimation
[56]	CNN	96	1	[–15, 15]	3GPP urban macro	CSI estimation
[57]	TDELM	64	1	—	Experimental data	CSI estimation
[59]	DNN	64 × 64	1	[0, 30]	Beamspace MIMO	CSI estimation
[60]	DNN	32	1	Noiseless	COST 2100	CSI compression
[61]	CNN	32	8	[0, 20]	Urban outdoor	Inter-BS CSI inference
[62]	DNN	128	1	25	Multipath	UL-to-DL CSI inference

3GPP: 3rd Generation Partnership Project; TDELM: Tucker decomposed extreme learning machine; COST: cooperation in science and technology; BS: base station; UL: uplink; DL: downlink.

than the signal power, the method presented by Neumann et al. achieves a spectral efficiency close to the theoretical upper bound. This is accomplished by designing a CNN that exploits a particular structure of the covariance matrix of conditionally normal channels. Numerical results showed that even when using other channel models such as the 3GPP urban macro model, the CNN outperformed other channel estimation methods of similar computational complexity.

Once CSI estimation has been performed, multiuser detection (MUD) algorithms distinguish the signals from different users transmitting simultaneously in a MIMO communication system. The maximum likelihood (MLH) detector yields optimal results, but the associated computational costs hinder its adoption in practical systems. As an alternative, the authors of [63] propose a method based on a GA that provides a tradeoff between the quality of service and computational costs. Comprehensive testing was performed by the authors of [64], who implemented joint CSI estimation and MUD with a variety of algorithms, including GA, PSO, and DE. Results indicate that these algorithms allow achieving optimal or almost optimal results but with a lower computational burden with respect to the MLH detector.

Blind identification of MIMO signals is the problem of identifying the MIMO schemes being used in a given environment. MIMO identification is of interest in the implementation of self-adapting cognitive radio networks and for electronic warfare applications [65]. In [66], an innovative approach based on MLP expands on the number of detectable MIMO schemes in orthogonal frequency-division multiplexing communication systems and is also able to estimate the number of transmitting antennas.

AI techniques have also been suitably applied to analog, digital, and hybrid beamforming in smart antenna arrays for MIMO communications. In this framework, a ML-based approach has been proposed in [67] aimed at coordinating a number of distributed base stations to simultaneously serve a mobile user for supporting highly mobile mm-wave applications with reliable coverage, low latency, and negligible training overhead. In [68], a two-stage scheme has been instead adopted in which, in the first stage, the digital precoding and combiner are switched on and off depending on the nature of the channel and, in the second stage, a ML assisted adaptation strategy is exploited for compensating the propagation losses. A different ML-based technique and situational awareness strategy have been combined in [69] to learn the beam information from past observations to reconfigure the antenna array and guarantee reliable mm-wave communications for vehicular applications.

ELEMENT FAILURES

One advantage of an antenna array is its graceful degradation in performance over time. In other words, an element failure results in a performance decrease but not a system failure. The performance decrease may be compensated by reconfiguring the array beamforming network.

The first step for dealing with failures in an array is to identify the defective elements. The problem of failure detection for a given array system has been widely covered in the literature. A number of different AI approaches have been proposed, including GA [70], [71], case-based reasoning (CBR) [72], SVM [73], and NN [74], [75].

Table 3 reports the main characteristics of the numerical simulations used to assess the performance of the failure detection methods. In the "Noise Type" column, it is possible to note that the numerical simulations employ either one of the following three kinds of measurement error: 1) AWGN applied to the measured pattern samples in linear scale, 2) a uniformly distributed noise applied on each pattern sample in linear scale, or 3) a uniformly distributed noise applied on each pattern sample in dB scale. The differences in the three error models prevent a fair comparison between the various failure detection methods. However, it is safe to conclude that the SVM- and CBR-based methods were tested in scenarios with the highest noise levels.

It is also possible to notice that GA-based strategies have received significant attention for failure detection. A possible explanation is that the elements of an array being diagnosed for

TABLE 3. A COMPARISON OF AI TECHNIQUES FOR FAILURE DETECTION.

Reference	AI Technique	Number of Elements	Failures (%)	Number of Pattern Measurements	Number of Pattern Measurements per Failure	Noise Type	Noise Strength
[70]	GA	8 × 8	4.69	20	6.67	Uniform, dB scale	Max ± 0.75 dB
[71]	GA	15 × 15	8.89	900	45	Uniform, linear scale	Max ± 10^{-5}
[72]	CBR	100	4	50	12.5	AWGN, linear scale	SNR = [0.5, 2] dB
[73]	SVM	4	50	19	9.5	AWGN, linear scale	SNR = [0, 25] dB
[74]	MLP	16	18.75	37	12.34	Noiseless	—
[75]	WL-NN	100	4	100	25	Uniform, dB scale	Max ± 0.2 dB

AWGN: additive white Gaussian noise; WLM: Woodward-Lawson method.

failures are easily represented with a string of binary variables, where "1" means "working" and "0" means "failed." Due to their inherent suitability for binary variables, GAs seem like a straightforward choice for the implementation of an optimization method based on such representation.

Most of the failure detection strategies considered were tested on arrays with a low percentage of failures, ranging between 4% and 18.75%. However, the SVM-based method described in [73] takes into consideration a failure rate of 50%. Even though this result refers to a small array, it is still remarkable since both the training and detection phases of the algorithm were performed on data with varying levels of noise and an SNR between 0 and 25 dB.

Once the defective elements have been identified, the remaining functioning elements can be reconfigured to compensate for the performance loss. The reconfigured weights are found using a GA [76] or other bioinspired algorithms [77]. If the direction of arrival of all the incoming signals is known, the algorithm reported in [78] reconstructs the received signal at the location of the faulty elements.

A different proactive approach to manage array failures is described in [79], where failure mitigation is ensured in the early stages of the array design process. In particular, a GA optimizes element weights to minimize the mismatch from a reference pattern not only in the case of normal operations but also in the event of element failure. The cost function weights the pattern error by the probability of failure. In the case of an eight-element GA-optimized array, the antenna maintains a radiation pattern similar to the reference one even in the case of failure of one element, as shown in Figure 10.

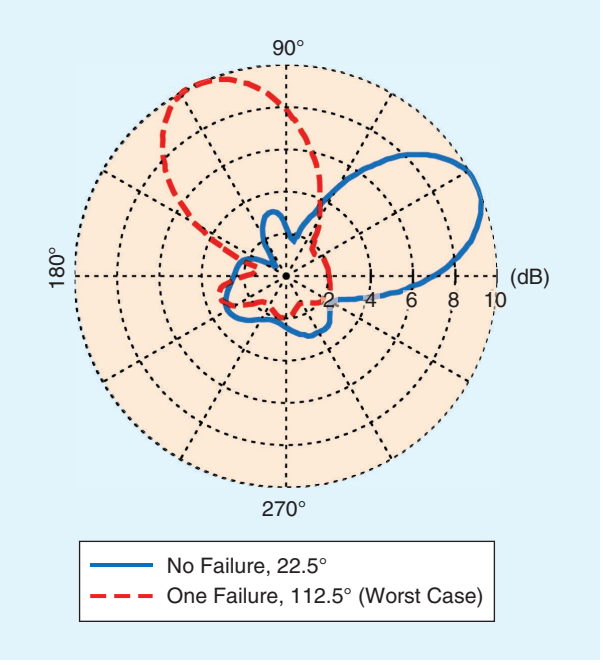

FIGURE 10. In the event of a failure, the GA-optimized array maintains good radiation characteristics [79].

ARRAY CALIBRATION

Antenna arrays require hardware calibration to avoid deviations in the radiated pattern and degraded performance. Calibration tables across the frequency band and scan range correct errors from a number of sources [13]. The thermal noise in array components, elements, and feed produces random amplitude and phase errors in signals. Component tolerances, frequency dependence, and beam scanning induce additional errors in the signals. Random failures, especially with mechanical components, cause additional errors. Adaptive and reconfigurable arrays are very sensitive to errors and require constant calibration (see the "Adaptive Nulling" section).

One array calibration approach (Figure 11) has a near-field planar scanner in front of the array under test [80]. A computer reads the measurements and updates the control codes of the array amplifiers and phase shifters in real time. A GA iterates to find the calibration table for the array. A binary GA works well with the binary controls for the amplifiers and phase shifters. This method was experimentally demonstrated on an eight-element array using different steering directions.

A phase calibration system for cylindrical parabolic reflector antennas with an array feed is presented in [81]. A GA was also used in this case. The GA operates on a set of continuous phase values, and the resulting values initialize a local optimizer

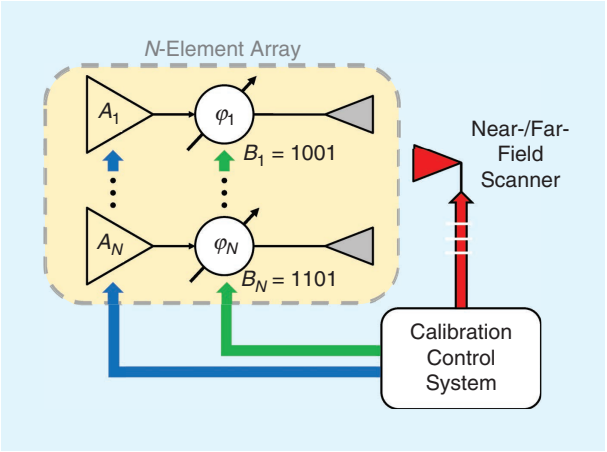

FIGURE 11. An automated array calibration system based on GAs [80].

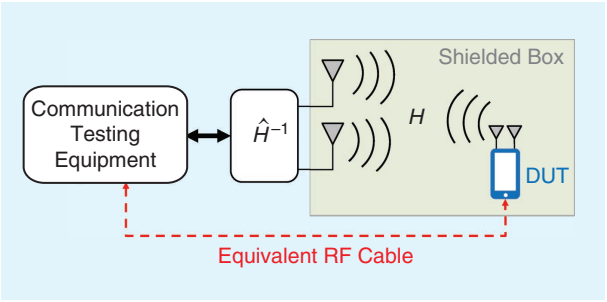

FIGURE 12. In the wireless cable method implementation of [83], a PSO estimates the inverse transfer matrix $\hat{H}^{-1}$ to enable a cable-like connection to the DUT.

operating over discrete values so as to take into account phase quantization errors.

ANNs have also found use in array calibration. In [82], a massive MIMO scheme with time division duplexing permits the use of the same channel for both downlink and uplink. Ideally, reciprocity holds between the transmitter and receiver, implying that the channel transfer function is the same in both directions. In reality, differences in the amplitude and phase of the RF chains of the two communicating devices upset reciprocity. An ANN with customized architecture in [82] calibrates the RF chains of both devices and restores channel reciprocity. The ANN approach has a simple hardware implementation and requires little computational power.

PSO was implemented in the "wireless cable" method for mobile terminal testing [83]. In the traditional testing setup, a base station emulator connects to the device under test (DUT) with physical cables and ports for each antenna. However, massive MIMO and mm-wave communications present increased antenna density, and the implementation of physical connectors make this setup impractical. The wireless cable method involves: 1) sending test signals directly to the desired antenna port over the air, and 2) compensating the transfer matrix H between the testing equipment and the DUT [84]. The authors of [83] implemented an experimental setup using the wireless cable method, as displayed in Figure 12, and employed a PSO to compute the transfer matrix $\hat{H}^{-1}$ that compensates the actual channel matrix. In this case, the PSO provides a solution that scales to a large number of antennas.

CONCLUSIONS

AI has many applications in adaptive and reconfigurable antenna arrays. This article presented array architectures important for implementing AI algorithms as well as five different example areas of research. AI approaches compete well with traditional approaches, often working in situations where other methods fail.

One major advantage of AI approaches is their ability to tackle large, nonlinear problems with many variables. Traditional signal processing algorithms tend to be local and work best with a small number of variables. Like humans, AI gives the algorithm the ability to "think" outside the limited box and the previous experience. Another advantage that AI offers is its robust performance in the presence of noise and multipath. Traditional methods struggle to maintain sufficient SNR or BER performance when confronted with realistic operating environments.

AI is "artificial" and needs human guidance and decision making for peak performance. Any adaptive or reconfigurable array controlled by AI ultimately must look to human judgment to avoid making costly mistakes. With the limits of AI in mind, the potential benefits of using AI in adaptive and reconfigurable arrays are well worth considering.

AUTHOR INFORMATION

Francesco Zardi (francesco.zardi@unitn.it) is with the ELEDIA@UniTN Research Center in the Department of Information Engineering and Computer Science, University of Trento, Italy. His research interests include the synthesis and design of antenna arrays and electromagnetic inverse scattering problems.

Payam Nayeri (pnayeri@mines.edu) is with the Department of Electrical Engineering, Colorado School of Mines, USA. His research interests include wideband antennas and arrays, adaptive beamforming, and reconfigurable microwave circuits. He is a Senior Member of IEEE.

Paolo Rocca (paolo.rocca@unitn.it) is an associate professor with the ELEDIA@UniTN Research Center in the Department of Information Engineering and Computer Science, University of Trento, Italy. His research interests include artificial intelligence techniques as applied to electromagnetics, antenna array design, and electromagnetic inverse scattering. He is a Senior Member of IEEE.

Randy L. Haupt (rhaupt@mines.edu) is a professor of electrical engineering at the Colorado School of Mines, USA. His research interests include antennas, phased arrays, smart antennas, genetic algorithms, and wireless communications. He is a Fellow of IEEE.

REFERENCES

[1] R. Monzingo, R. Haupt, and T. Miller, *Introduction to Adaptive Arrays*. Raleigh, NC: SciTech Pub., 2011.

[2] R. L. Haupt and M. Lanagan, "Reconfigurable antennas," *IEEE Antennas Propag. Mag.*, vol. 55, no. 1, pp. 49–61, Feb. 2013. doi: 10.1109/MAP.2013.6474484.

[3] P. Stone et al., "Artificial intelligence and life in 2030: One hundred year study on artificial intelligence," Stanford Univ., CA, Sept. 2016. Accessed: Jan. 29, 2020. [Online]. Available: http://ai100.stanford.edu/2016-report

[4] "Artificial intelligence IEEE Position Statement, approved by the IEEE Board of Directors," Piscataway, NJ, June 2019. Accessed: June 26, 2020. [Online]. Available: https://globalpolicy.ieee.org/wp-content/uploads/2019/06/IEEE18029.pdf

[5] "Machine learning," IEEE Systems, Man, and Cybernetics Society, Piscataway, NJ. Accessed: Jan. 29, 2020. [Online]. Available: http://www.ieeesmc.org/technical-activities/cybernetics/machine-learning

[6] M. Harris, "NTSB investigation into deadly Uber self-driving car crash reveals lax attitude toward safety," *IEEE Spectrum*, Nov. 7, 2019. Accessed: Jan. 29, 2020. [Online]. Available: https://spectrum.ieee.org/cars-that-think/transportation/self-driving/ntsb-investigation-into-deadly-uber-selfdriving-car-crash-reveals-lax-attitude-toward-safety

[7] P. Aksenov, "Stanislav Petrov: The man who may have saved the world," BBC.com. Accessed: Jan. 29, 2020. [Online]. https://www.bbc.com/news/world-europe-24280831

[8] D. E. Goldberg, *Genetic Algorithms in Search Optimization and Machine Learning*, New York: Addison-Wesley, 1989.

[9] J. Kennedy and R. Eberhart, "Particle swarm optimization," in *Proc. Int. Conf. Neural Netw. (ICNN'95)*, Perth, WA, 1995, vol. 4, pp. 1942–1948. doi: 10.5772/intechopen.89633.

[10] S. Kirkpatrick, C. D. Gelatt, and M. P. Vecchi, "Optimization by simulated annealing," *Science*, vol. 220, no. 4598, pp. 671–680, May 1983. doi: 10.1126/science.220.4598.671.

[11] I. Goodfellow, Y. Bengio, and A. Courville, *Deep Learning*. Cambridge, MA: MIT Press, 2017.

[12] A. Massa, D. Marcantonio, X. Chen, M. Li, and M. Salucci, "DNNs as applied to electromagnetics, antennas, and propagation – A review," *IEEE Antennas Wireless Propag. Lett.*, vol. 18, no. 11, pp. 2225–2229, Nov. 2019. doi: 10.1109/LAWP.2019.2916369.

[13] R. L. Haupt, *Timed Arrays Wideband and Time Varying Antenna Arrays*. Hoboken, NJ: Wiley, 2015.

[14] P. Barton, "Digital beam forming for radar," *IEE Proc. F, Commun., Radar Signal Process.*, vol. 127, no. 4, pp. 266–277, Aug. 1980. doi: 10.1049/ip-f-1.1980.0041.

[15] H. Steyskal, "Digital beamforming antennas – An introduction," *Microw. J.*, vol. 30, no. 1, pp. 107–124, Jan. 1987. doi: 10.1109/EUMA.1988.333796.

[16] R. L. Haupt, *Antenna Arrays: A Computational Approach*, Hoboken, NJ: Wiley, 2010.

[17] A. Akindoyin, M. Willerton, and A. Manikas, "Localization and array shape estimation using software defined radio array testbed," in *Proc. IEEE Sensor Array and Multichannel Signal Process. Workshop (SAM)*, 2014, pp. 189–192. doi: 10.1109/SAM.2014.6882372.

[18] P. Nayeri and R. L. Haupt, "A testbed for adaptive beamforming with software defined radio arrays," in *Proc. IEEE/ACES Int. Conf. Wireless Inf. Technol. Syst. (ICWITS) Appl. Comput. Electromag. (ACES)*, Honolulu, HI, 2016, pp. 1–2. doi: 10.1109/ROPACES.2016.7465449.

[19] C. Campo, M. Stefer, L. Bernard, S. Hengy, H. Boeglen, and J. M. Paillot, "Antenna weighting system for a uniform linear array based on software defined radio," in *Proc. Mediterranean Microw. Symp. (MMS)*, 2017, pp. 1–4. doi: 10.1109/MMS.2017.8497138.

[20] R. L. Haupt, "Phase-only adaptive nulling with genetic algorithms," *IEEE Trans. Antennas Propag.*, vol. 45, no. 6, pp. 1009–1015, June 1997. doi: 10.1109/8.585749.

[21] R. L. Haupt and H. L. Southall, "Experimental adaptive nulling with a genetic algorithm," *Microw. J.*, vol. 42, no. 1, pp. 78–89, Jan. 1999.

[22] D. Gaydos, P. Nayeri and R. Haupt, "Experimental demonstration of a software-defined-radio adaptive beamformer," in *Proc. European Radar Conf. (EuRAD)*, Madrid, 2018, pp. 561–564. doi: 10.23919/EuRAD.2018.8546564.

[23] P. Nayeri and R. Haupt, "A comparison of digital beamforming and power minimization adaptive nulling algorithms using a software defined radio antenna array," in *Proc. IEEE Int. Symp. Antennas Propag. & USNC/URSI Nat. Radio Sci. Meet.*, Boston, 2018, pp. 7–8. doi: 10.1109/APUSNCURSINRSM.2018.8608839.

[24] D. Gaydos, P Nayeri, and R Haupt, "Experimental comparison of digital beamforming interference cancellation algorithms using a software defined radio array," in *Proc. United States Nat. Committee URSI Nat. Radio Sci. Meet. (USNC-URSI NRSM)*, Boulder, CO, Jan. 2019, pp. 1–2. doi: 10.23919/USNC-URSI-NRSM.2019.8712925.

[25] D. Gaydos, P. Nayeri, and R. Haupt, "Adaptive beamforming in high-interference environments using a software-defined radio array," in *Proc. IEEE Int. Symp. Antennas Propag. & USNC/URSI Nat. Radio Sci. Meeting*, Atlanta, GA, July 2019, pp. 1501–1502. doi: 10.1109/APUSNCURSINRSM.2019.8888670.

[26] A. Akindoyin, M. Willerton and A. Manikas, "Localization and array shape estimation using software defined radio array testbed," in *Proc. IEEE Sensor Array and Multichannel Sig. Proc. Workshop*, 2014, pp. 189–192. doi: 10.1109/SAM.2014.6882372.

[27] Z. Farid, R. Nordin, and M. Ismail, "Recent advances in wireless indoor localization techniques and systems," *J. Comput. Netw. Commun.*, vol. 2013, pp. 1–12, Sept. 2013. doi: 10.1155/2013/185138.

[28] R. Schmidt, "Multiple emitter location and signal parameter estimation," *IEEE Trans. Antennas Propag.*, vol. 34, no. 3, pp. 276–280, Mar. 1986. doi: 10.1109/TAP.1986.1143830.

[29] R. Roy and T. Kailath, "ESPRIT-estimation of signal parameters via rotational invariance techniques," *IEEE Trans. Acoust.*, vol. 37, no. 7, pp. 984–995, July 1989. doi: 10.1109/29.32276.

[30] H. L. Southall, J. A. Simmers, and T. H. O'Donnell, "Direction finding in phased arrays with a neural network beamformer," *IEEE Trans. Antennas Propag.*, vol. 43, no. 12, pp. 1369–1374, 1995. doi: 10.1109/8.475924.

[31] Z. Liu, C. Zhang, and P. S. Yu, "Direction-of-arrival estimation based on deep neural networks with robustness to array imperfections," *IEEE Trans. Antennas Propag.*, vol. 66, no. 12, pp. 7315–7327, Dec. 2018. doi: 10.1109/TAP.2018.2874430.

[32] H. Xiang, B. Chen, M. Yang, and C. Li, "Altitude measurement based on characteristics reversal by deep neural network for VHF radar," *IET Radar, Sonar Navig.*, vol. 13, no. 1, pp. 98–103, Jan. 2019. doi: 10.1049/iet-rsn.2018.5121.

[33] M. Donelli, F. Viani, P. Rocca, and A. Massa, "An innovative multiresolution approach for DoA estimation based on a support vector classification," *IEEE Trans. Antennas Propag.*, vol. 57, no. 8, pp. 2279–2292, Aug. 2009. doi: 10.1109/TAP.2009.2024485.

[34] K. C. Sharman, "Maximum likelihood parameter estimation by simulated annealing," in *Proc. Int. Conf. Acoust., Speech, Signal Process. (ICASSP-88)*, New York, 1988, pp. 2741–2744. doi: 10.1109/ICASSP.1988.197217.

[35] N. J. G. Fonseca, M. Coudyser, J. Laurin, and J. Brault, "On the design of a compact neural network-based DoA estimation system," *IEEE Trans. Antennas Propag.*, vol. 58, no. 2, pp. 357–366, Feb. 2010. doi: 10.1109/TAP.2009.2037766.

[36] J. Fuchs, R. Weigel, and M. Gardill, "Single-snapshot direction-of-arrival estimation of multiple targets using a multi-layer perceptron," in *Proc. IEEE MTT-S Int. Conf. Microw. Intell. Mobility (ICMIM)*, Detroit, MI, 2019, pp. 1–4.

[37] K. A. Gotsis, K. Siakavara, and J. N. Sahalos, "On the direction of arrival (DoA) estimation for a switched-beam antenna system using neural networks," *IEEE Trans. Antennas Propag.*, vol. 57, no. 5, pp. 1399–1411, May 2009. doi: 10.1109/TAP.2009.2016721.

[38] H. Huang, J. Yang, H. Huang, Y. Song, and G. Gui, "Deep learning for super-resolution channel estimation and DoA estimation based massive MIMO system," *IEEE Trans. Veh. Technol.*, vol. 67, no. 9, pp. 8549–8560, Sept. 2018. doi: 10.1109/TVT.2018.2851783.

[39] C.-S. Shieh and C.-T. Lin, "Direction of arrival estimation based on phase differences using neural fuzzy network," *IEEE Trans. Antennas Propag.*, vol. 48, no. 7, pp. 1115–1124, July 2000. doi: 10.1109/8.876331.

[40] S. Jha and T. Durrani, "Direction of arrival estimation using artificial neural networks," *IEEE Trans. Syst. Man. Cybern.*, vol. 21, no. 5, pp. 1192–1201, Sept.–Oct. 1991. doi: 10.1109/21.120069.

[41] M. Agatonovic, Z. Stanković, and B. Milovanović, "High resolution two-dimensional DOA estimation using artificial neural networks," in *Proc. European Conf. Antennas Propag. (EUCAP)*, Prague, 2012, pp. 1–5.

[42] T. Lo, H. Leung, and J. Litva, "Radial basis function neural network for direction-of-arrivals estimation," *IEEE Signal Process. Lett.*, vol. 1, no. 2, pp. 45–47, Feb. 1994. doi: 10.1109/97.300315.

[43] A. Khan, S. Wang, and Z. Zhu, "Angle-of-arrival estimation using an adaptive machine learning framework," *IEEE Commun. Lett.*, vol. 23, no. 2, pp. 294–297, Feb. 2019. doi: 10.1109/LCOMM.2018.2884464.

[44] A. Massa, G. Oliveri, M. Salucci, N. Anselmi, and P. Rocca, "Learning-by-examples techniques as applied to electromagnetics," *J. Electromagn. Waves Appl.*, vol. 32, no. 4, pp. 516–541, 2018. doi: 10.1080/09205071.2017.1402713.

[45] F. Viani, M. Donelli, M. Salucci, P. Rocca, and A. Massa, "Opportunistic exploitation of wireless infrastructures for homeland security," in *Proc. IEEE Int. Symp. Antennas Propag. (APSURSI)*, 2011, pp. 3062–3065.

[46] Y. Ma et al., "An image-aware based smart antenna capable of automatic beam switching for indoor mobile communication," *IEEE Access*, vol. 8, pp. 379–388, 2020. doi: 10.1109/ACCESS.2019.2961379.

[47] H. A. Nguyen, H. Guo, and K. Low, "Real-time estimation of sensor node's position using particle swarm optimization with log-barrier constraint," *IEEE Trans. Instrum. Meas.*, vol. 60, no. 11, pp. 3619–3628, Nov. 2011. doi: 10.1109/TIM.2011.2135030.

[48] Z. Wu, K. Fu, E. Jedari, S. R. Shuvra, R. Rashidzadeh, and M. Saif, "A fast and resource efficient method for indoor positioning using received signal

strength," *IEEE Trans. Veh. Technol.*, vol. 65, no. 12, pp. 9747–9758, Dec. 2016. doi: 10.1109/TVT.2016.2530761.
[49] X. Wang, L. Gao, and S. Mao, "CSI phase fingerprinting for indoor localization with a deep learning approach," *IEEE Internet Things J.*, vol. 3, no. 6, pp. 1113–1123, Dec. 2016. doi: 10.1109/JIOT.2016.2558659.
[50] X. Sun, C. Wu, X. Gao, and G. Y. Li, "Fingerprint-based localization for massive MIMO-OFDM system with deep convolutional neural networks," *IEEE Trans. Veh. Technol.*, vol. 68, no. 11, pp. 10,846–10,857, Nov. 2019. doi: 10.1109/TVT.2019.2939209.
[51] F. Viani, P. Rocca, M. Benedetti, G. Oliveri, and A. Massa, "Electromagnetic passive localization and tracking of moving targets in a WSN-infrastructured environment," *Inv. Prob.*, vol. 26, no. 7, pp. 1–15, Mar. 2010.
[52] L. Zhao, H. Huang, X. Li, S. Ding, H. Zhao, and Z. Han, "An accurate and robust approach of device-free localization with convolutional autoencoder," *IEEE Internet Things J.*, vol. 6, no. 3, pp. 5825–5840, June 2019. doi: 10.1109/JIOT.2019.2907580.
[53] J. Liang, C. S. Leung, and H. C. So, "Lagrange programming neural network approach for target localization in distributed MIMO radar," *IEEE Trans. Signal Process.*, vol. 64, no. 6, pp. 1574–1585, Mar. 2016. doi: 10.1109/TSP.2015.2500881.
[54] C. Chun, J. Kang, and I. Kim, "Deep learning-based channel estimation for massive MIMO systems," *IEEE Wireless Commun. Lett.*, vol. 8, no. 4, pp. 1228–1231, Aug. 2019. doi: 10.1109/LWC.2019.2912378.
[55] Y. Jin, J. Zhang, S. Jin, and B. Ai, "Channel estimation for cell-free mmwave massive MIMO through deep learning," *IEEE Trans. Veh. Technol.*, vol. 68, no. 10, pp. 10,325–10,329, Oct. 2019. doi: 10.1109/TVT.2019.2937543.
[56] D. Neumann, T. Wiese, and W. Utschick, "Learning the MMSE channel estimator," *IEEE Trans. Signal Process.*, vol. 66, no. 11, pp. 2905–2917, June 2018. doi: 10.1109/TSP.2018.2799164.
[57] H. Zhang, B. Ai, W. Xu, L. Xu, and S. Cui, "Multi-antenna channel interpolation via tucker decomposed extreme learning machine," *IEEE Trans. Veh. Technol.*, vol. 68, no. 7, pp. 7160–7163, July 2019. doi: 10.1109/TVT.2019.2913865.
[58] J. Brady, N. Behdad, and A. M. Sayeed, "Beamspace MIMO for millimeter-wave communications: System architecture, modeling, analysis, and measurements," *IEEE Trans. Antennas Propag.*, vol. 61, no. 7, pp. 3814–3827, July 2013. doi: 10.1109/TAP.2013.2254442.
[59] H. He, C. Wen, S. Jin, and G. Y. Li, "Deep learning-based channel estimation for beamspace mmWave massive MIMO systems," *IEEE Wireless Commun. Lett.*, vol. 7, no. 5, pp. 852–855, Oct. 2018. doi: 10.1109/LWC.2018.2832128.
[60] C. Wen, W. Shih, and S. Jin, "Deep learning for massive MIMO CSI feedback," *IEEE Wireless Commun. Lett.*, vol. 7, no. 5, pp. 748–751, Oct. 2018. doi: 10.1109/LWC.2018.2818160.
[61] S. Chen et al., "Learning-based remote channel inference: Feasibility analysis and case study," *IEEE Trans. Wirel. Commun.*, vol. 18, no. 7, pp. 3554–3568, July 2019. doi: 10.1109/TWC.2019.2915683.
[62] Y. Yang, F. Gao, G. Y. Li, and M. Jian, "Deep learning-based downlink channel prediction for FDD massive MIMO system," *IEEE Commun. Lett.*, vol. 23, no. 11, pp. 1994–1998, Nov. 2019. doi: 10.1109/LCOMM.2019.2934851.
[63] M. Y. Alias, S. Chen, and L. Hanzo, "Multiple-antenna-aided OFDM employing genetic-algorithm-assisted minimum bit error rate multiuser detection," *IEEE Trans. Veh. Technol.*, vol. 54, no. 5, pp. 1713–1721, Sept. 2005. doi: 10.1109/TVT.2005.851303.
[64] J. Zhang, S. Chen, X. Mu, and L. Hanzo, "Evolutionary-algorithm-assisted joint channel estimation and turbo multiuser detection/decoding for OFDM/SDMA," *IEEE Trans. Veh. Technol.*, vol. 63, no. 3, pp. 1204–1222, Mar. 2014. doi: 10.1109/TVT.2013.2283069.
[65] Y. A. Eldemerdash, O. A. Dobre, and M. Öner, "Signal Identification for multiple-antenna wireless systems: Achievements and challenges," *IEEE Commun. Surv. Tut.*, vol. 18, no. 3, pp. 1524–1551, 2016. doi: 10.1109/COMST.2016.2519148.
[66] M. Gao, Y. Li, O. A. Dobre, and N. Al-Dhahir, "Joint blind identification of the number of transmit antennas and MIMO schemes using Gerschgorin radii and FNN," *IEEE Trans. Wireless Commun.*, vol. 18, no. 1, pp. 373–387, Jan. 2019. doi: 10.1109/TWC.2018.2879941.
[67] A. Alkhateeb, S. Alex, P. Varkey, Y. Li, Q. Qu, and D. Tujkovic, "Deep learning coordinated beamforming for highly-mobile millimeter wave systems," *IEEE Access*, vol. 6, pp. 37,328–37,348, June 2018. doi: 10.1109/ACCESS.2018.2850226.
[68] K. Satyanarayana, M. El-Hajjar, A. A. M. Mourad, and L. Hanzo, "Multi-user hybrid beamforming relying on learning-aided link-adaptation for mmwave systems," *IEEE Access*, vol. 7, pp. 23,197–23,209, Feb. 2019. doi: 10.1109/ACCESS.2019.2900008.
[69] Y. Wang, M. Narasimha, and R. W. Heath, "MmWave beam prediction with situational awareness: A machine learning approach," in *Proc. IEEE 19th Int. Workshop Signal Process. Adv. Wireless Commun. (SPAWC)*, Kalamata, 2018, pp. 1–5. doi: 10.1109/SPAWC.2018.8445969.
[70] J. A. Rodriguez, F. Ares, H. Palacios, and J. Vassal'lo, "Finding defective elements in planar arrays using genetic algorithms," *Progress Electromagn. Res.*, vol. 29, pp. 25–37, 2000. doi: 10.2528/PIER00011401.
[71] O. M. Bucci, A. Capozzoli, and G. D'Elia, "Diagnosis of array faults from far-field amplitude-only data," *IEEE Trans. Antennas Propag.*, vol. 48, no. 5, pp. 647–652, May 2000. doi: 10.1109/8.855482.
[72] R. Iglesias, F. Ares, M. Fernandez-Delgado, J. A. Rodriguez, J. Bregains, and S. Barro, "Element failure detection in linear antenna arrays using case-based reasoning," *IEEE Trans. Antennas Propag.*, vol. 50, no. 4, pp. 198–204, Aug. 2008. doi: 10.1109/MAP.2008.4653709.
[73] N. Xu, C. G. Christodoulou, S. E. Barbin and M. Martinez-Ramon, "Detecting failure of antenna array elements using machine learning optimization," in *Proc. IEEE Antennas Propag. Soc. Int. Symp.*, Honolulu, HI, June 2007, pp. 5753–5756.
[74] A. Patnaik, B. Choudhury, P. Pradhan, R. K. Mishra, and C. Christodoulou, "An ANN application for fault finding in antenna arrays," *IEEE Trans. Antennas Propag.*, vol. 55, no. 3, pp. 775–777, Mar. 2007. doi: 10.1109/TAP.2007.891557.
[75] J. A. Rodriguez, M. Fernandez-Delgado, J. Bregains, R. Iglesias, S. Barro and F. Ares, "A comparison among several techniques for finding defective elements in antenna arrays," in *Proc. 2nd Eur. Conf. Antennas Propag., EuCAP 2007*, Edinburgh, Nov. 2007, pp. 1–8. doi: 10.1049/ic.2007.1141.
[76] B.-K. Yeo and Y. Lu, "Array failure correction with a genetic algorithm," *IEEE Trans. Antennas Propag.*, vol. 47, no. 5, pp. 823–828, May 1999. doi: 10.1109/8.774136.
[77] O. P. Acharya, A. Patnaik, and S. N. Sinha, "Comparative study of bio-inspired optimization techniques in antenna array failure compensation," in *Proc. IEEE Int. Symp. Antennas Propag. (APSURSI)*, Orlando, FL, 2013, pp. 1232–1233. doi: 10.1109/APS.2013.6711276.
[78] H. Steyskal and R. J. Mailloux, "Generalisation of an array-failure-correction method," *Proc. Inst. Elect. Eng.-Microw. Antennas Propag.*, vol. 145, no. 4, pp. 332–336, 1998. doi: 10.1049/ip-map:19982059.
[79] S. A. Mitilineos, S. C. A. Thomopoulos, and C. N. Capsalis, "On array failure mitigation with respect to probability of failure, using constant excitation coefficients and a genetic algorithm," *IEEE Antennas Wireless Propag. Lett.*, vol. 5, pp. 187–190, May 2006. doi: 10.1109/LAWP.2006.874068.
[80] H.-T. Chou and D.-Y. Cheng, "Beam-pattern calibration in a realistic system of phased-array antennas via the implementation of a genetic algorithm with a measurement system," *IEEE Trans. Antennas Propag.*, vol. 65, no. 2, pp. 593–601, Feb. 2017. doi: 10.1109/TAP.2016.2635630.
[81] R. L. Haupt, "Calibration of cylindrical reflector antennas with linear phased array feeds," *IEEE Trans. Antennas Propag.*, vol. 56, no. 2, pp. 593–596, 2008. doi: 10.1109/TAP.2007.915489.
[82] C. Shan, X. Chen, H. Yin, W. Wang, G. Wei, and Y. Zhang, "Diagnosis of calibration state for massive antenna array via deep learning," *IEEE Wireless Commun. Lett.*, vol. 8, no. 5, pp. 1431–1434, Oct. 2019. doi: 10.1109/LWC.2019.2920818.
[83] W. Fan, F. Zhang, P. Kyösti, L. Hentilä, and G. F. Pedersen, "Wireless cable method for high-order mimo terminals based on particle swarm optimization algorithm," *IEEE Trans. Antennas Propag*, vol. 66, no. 10, pp. 5536–5545, Oct. 2018. doi: 10.1109/TAP.2018.2858193.
[84] W. Fan, P. Kyösti, L. Hentilä, and G. F. Pedersen, "MIMO terminal performance evaluation with a novel wireless cable method," *IEEE Trans. Antennas Propag.*, vol. 65, no. 9, pp. 4803–4814, Sept. 2017. doi: 10.1109/TAP.2017.2723260.